



Minerva Access is the Institutional Repository of The University of Melbourne

Author/s:

Mito, R;Pedersen, M;Pardoe, H;Parker, D;Smith, RE;Cameron, J;Scheffer, IE;Berkovic, SF;Vaughan, DN;Jackson, GD

Title:

Exploring individual fixel-based white matter abnormalities in epilepsy

Date:

2024-01-01

Citation:

Mito, R., Pedersen, M., Pardoe, H., Parker, D., Smith, R. E., Cameron, J., Scheffer, I. E., Berkovic, S. F., Vaughan, D. N. & Jackson, G. D. (2024). Exploring individual fixel-based white matter abnormalities in epilepsy. *Brain Communications*, 6 (1), <https://doi.org/10.1093/braincomms/fcad352>.

Persistent Link:




<https://hdl.handle.net/11343/344361>

License:

[CC BY](#)

# BRAIN COMMUNICATIONS

## Exploring individual fixel-based white matter abnormalities in epilepsy

 Remika Mito,<sup>1,2</sup> Mangor Pedersen,<sup>1,3</sup> Heath Pardoe,<sup>1</sup> Donna Parker,<sup>1</sup> Robert E. Smith,<sup>1,2</sup> Jillian Cameron,<sup>4</sup> Ingrid E. Scheffer,<sup>4</sup>  Samuel F. Berkovic,<sup>4</sup> David N. Vaughan<sup>1,2,5</sup> and  Graeme D. Jackson<sup>1,2,5</sup>

Diffusion MRI has provided insight into the widespread structural connectivity changes that characterize epilepsies. Although syndrome-specific white matter abnormalities have been demonstrated, studies to date have predominantly relied on statistical comparisons between patient and control groups. For diffusion MRI techniques to be of clinical value, they should be able to detect white matter microstructural changes in individual patients. In this study, we apply an individualized approach to a technique known as fixel-based analysis, to examine fibre-tract-specific abnormalities in individuals with epilepsy. We explore the potential clinical value of this individualized fixel-based approach in epilepsy patients with differing syndromic diagnoses. Diffusion MRI data from 90 neurologically healthy control participants and 10 patients with epilepsy (temporal lobe epilepsy, progressive myoclonus epilepsy, and Dravet Syndrome, malformations of cortical development) were included in this study. Measures of fibre density and cross-section were extracted for all participants across brain white matter fixels, and mean values were computed within select tracts-of-interest. Scanner harmonized and normalized data were then used to compute Z-scores for individual patients with epilepsy. White matter abnormalities were observed in distinct patterns in individual patients with epilepsy, both at the tract and fixel level. For patients with specific epilepsy syndromes, the detected white matter abnormalities were in line with expected syndrome-specific clinical phenotypes. In patients with lesional epilepsies (e.g. hippocampal sclerosis, periventricular nodular heterotopia, and bottom-of-sulcus dysplasia), white matter abnormalities were spatially concordant with lesion location. This proof-of-principle study demonstrates the clinical potential of translating advanced diffusion MRI methodology to individual-patient-level use in epilepsy. This technique could be useful both in aiding diagnosis of specific epilepsy syndromes, and in localizing structural abnormalities, and is readily amenable to other neurological disorders. We have included code and data for this study so that individualized white matter changes can be explored robustly in larger cohorts in future work.

- 1 Florey Institute of Neuroscience and Mental Health, Heidelberg, Victoria 3084, Australia
- 2 Florey Department of Neuroscience and Mental Health, University of Melbourne, Melbourne, Victoria 3010, Australia
- 3 Department of Psychology and Neuroscience, Auckland University of Technology (AUT), Auckland 1142, New Zealand
- 4 Epilepsy Research Centre, Department of Medicine, University of Melbourne, Austin Health, Heidelberg, Victoria 3084, Australia
- 5 Department of Neurology, Austin Health, Heidelberg, Victoria 3084, Australia

Correspondence to: Remika Mito  
Florey Institute of Neuroscience and Mental Health,  
245 Burgundy Street  
Heidelberg, Victoria 3084, Australia  
E-mail: [remika.mito@florey.edu.au](mailto:remika.mito@florey.edu.au)

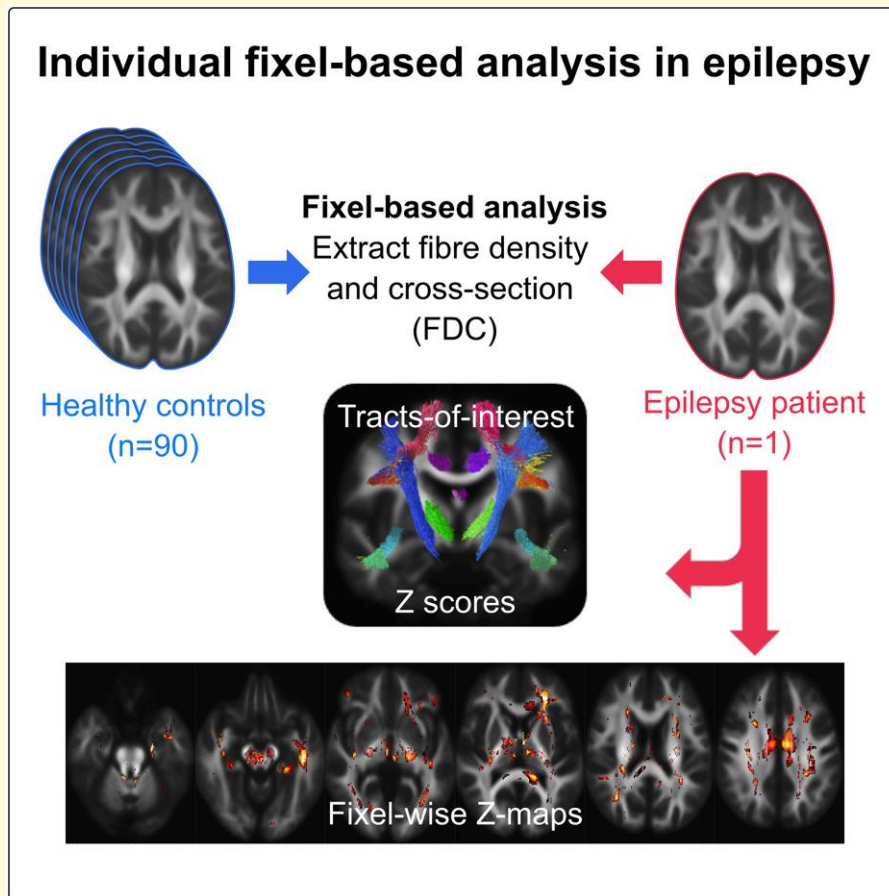
**Keywords:** epilepsy; diffusion MRI; fixel-based analysis; white matter; individual analysis

Received April 11, 2023. Revised November 02, 2023. Accepted December 21, 2023. Advance access publication December 22, 2023

© The Author(s) 2023. Published by Oxford University Press on behalf of the Guarantors of Brain.

This is an Open Access article distributed under the terms of the Creative Commons Attribution License (<https://creativecommons.org/licenses/by/4.0/>), which permits unrestricted reuse, distribution, and reproduction in any medium, provided the original work is properly cited.

## Graphical Abstract



## Introduction

Epilepsy is widely considered a network disorder, with hyperexcitability and hypersynchrony within brain networks driving disturbance in brain function.<sup>1</sup> Although the study of brain network disturbances in epilepsy has predominantly focused on abnormal functional connectivity, there is growing interest in changes to the brain's structural connections, which likely subserve these functional network disruptions. Indeed, both focal and generalized epilepsies have been shown to exhibit widespread abnormalities in white matter (WM) fibre pathways, and these structural network disruptions are now understood to be a key characteristic of the epilepsies.<sup>1,2</sup>

Diffusion MRI or diffusion-weighted imaging (DWI) is currently the only tool available to noninvasively probe the *in vivo* WM architecture of the brain and has played a crucial role in untangling structural network changes in epilepsy. Diffusion MRI studies have revealed syndrome-specific patterns of WM alterations, both within predefined cohorts,<sup>3-6</sup> and across large consortia studies.<sup>2</sup> These WM changes appear clinically meaningful, as they are associated with cognitive function<sup>7,8</sup> and postsurgical outcome.<sup>9,10</sup> In epilepsy

patients with focal brain abnormalities, diffusion MRI measures may also help to localize epileptogenic lesions.<sup>11,12</sup>

Over the past two decades, major technical advancements in diffusion MRI have brought the corresponding potential for clinical utility in epilepsy. Yet, in clinical practice, the use of this technique is limited to a few well-defined applications; for example, to identify and avoid the optic radiation or corticospinal tract (CST) when planning surgical interventions in focal epilepsy.<sup>13</sup> This could be attributed to diffusion MRI studies in epilepsy being predominantly focused on group analyses, comparing patient cohorts with control cohorts. These group-level studies are inherently desensitized to individual patient differences, where clinical value is likely to be derived. For advanced neuroimaging techniques to be valuable in clinical practice, they must provide biologically and clinically meaningful information about individuals.

Unfortunately, there are challenges in translating diffusion MRI methods into individual-patient use. First, DWI metrics often relate to features of the observed diffusion process rather than direct properties of the underlying biology, such that clinical interpretation is often difficult.<sup>14,15</sup> Second, the detection of individual-level changes in neuroimaging-derived measures is hampered by the multiple

**Table 1** Clinical characteristics of epilepsy patients included in study

Patient	Sex	Age range at scan (years)	Epilepsy syndrome or cause	Lesion location	Age at seizure onset (years)
1	M	26–30	L TLE-HS	L temporal lobe	6–10
2	F	41–45	R TLE-HS	R temporal lobe	6–10
3	M	16–20	R TLE-LN	-	16–20
4	F	26–30	L TLE-LN	-	11–15
5	M	26–30	PME	-	11–15
6	M	26–30	Dravet	-	0–5
7	F	41–45	PVNH	L lateral ventricles	6–10
8	M	21–25	PVNH + PMG	Right ventricular/temporal	16–20
9	M	16–20	BOSD	R precentral sulcus	0–5
10	F	16–20	BOSD	R post-central sulcus	11–15

BOSD, bottom-of-sulcus dysplasia; PME, progressive myoclonus epilepsy; PMG, polymicrogyria; PVNH, periventricular nodular heterotopia; TLE-HS, temporal lobe epilepsy with hippocampal sclerosis; TLE-LN, lesion-negative temporal lobe epilepsy. Age ranges are provided for participants (5-year age range).

comparison problem when using classical statistical frameworks. Finally, the generalizability of diffusion MRI measures is difficult, given that their values depend on factors such as acquisition site and scanning protocol.<sup>16–18</sup>

In this study, we apply the fixel-based analysis (FBA) framework at the individual-patient level, to examine WM fibre-tract-specific changes in individuals with epilepsy. Unlike the more commonly used voxel-averaged measures derived from techniques like diffusion tensor imaging (DTI), FBA involves modelling of multiple fibre orientations within a voxel,<sup>19,20</sup> such that derived measures are both sensitive and specific to individual fibre orientations within a voxel. This provides more biologically interpretable measures of WM fibre-tract changes than can DTI, particularly in crossing-fibre voxels that constitute the majority of brain WM.<sup>21</sup>

Here, we provide the first (to our knowledge) individualized framework for FBA, and examine fibre-tract-specific changes in individuals with various causes of epilepsy. We provide means to quantify and visualize individual-level tract changes and incorporate data harmonization approaches into the fixel-based framework, including code and data for further exploration. We demonstrate clinically meaningful changes in individual epilepsy patients, which could be useful in the clinical work-up of syndromic epilepsies, and in localizing small epileptogenic lesions.

## Materials and methods

### Participants

Ten individuals with epilepsy were included in this study: two patients with temporal lobe epilepsy (TLE) and hippocampal sclerosis (HS); two patients with MRI-negative TLE; two patients with focal cortical dysplasia (bottom of the sulcus dysplasia); two patients with periventricular nodular heterotopia (PVNH) [one who had additional polymicrogyria (PMG)]; one patient with Dravet's syndrome; and one patient with progressive myoclonic epilepsy. People with epilepsy were recruited through the Austin Health Comprehensive Epilepsy Program, the first seizure clinic and/or neurology department at Austin Health and had a confirmed diagnosis of epilepsy. Patients were selected from previous imaging studies where

we performed group comparisons between patients with specific epilepsy syndromes or causes and control participants. For this proof-of-principle study, we selected patients who exhibited clinical signs that were representative of the particular syndrome or cause of epilepsy, rather than patients who showed complex aetiology. Clinical data for each patient included in this study is available in Table 1.

Ninety control participants were included in the normative sample. Control participants were adults [mean age: 36.9 years ( $\pm$ 13.3), range: 18–64 years] who had no history of seizures, psychiatric illness, or significant head injury. Age histograms for the healthy control cohort are provided in the [Supplementary Material \(Supplementary Fig. 1\)](#).

Written informed consent was provided by all participants or their parents/guardians. The study was approved by the Austin Health Human Research Ethics Committee.

### MRI data

All participants underwent an MRI scan at the Florey Institute of Neuroscience and Mental Health. MRI data were acquired at 3 T either on a 3 T Siemens Skyra or 3 T Siemens Tim Trio between 2011 and 2019.

DWI data were acquired on the Skyra with a 20-channel head coil receiver, with the following parameters: 60 axial slices, TR/TE (repetition time/time to echo) = 8400/110 ms, 2.5 mm isotropic voxels, in-plane parallel acceleration factor 2, 64 diffusion-weighted images ( $b = 3000 \text{ s/mm}^2$ ) and at least 1  $b = 0$  image. Equivalent DWI was acquired on a Siemens Tim Trio with a 12-channel head coil receiver with the following parameters: 60 axial slices, TR/TE = 8300/110 ms, 2.5 mm isotropic voxels, in-plane parallel acceleration factor 2, 60 diffusion-weighted images ( $b = 3000 \text{ s/mm}^2$ ) and 8  $b = 0$  images. A reverse phase-encoded  $b = 0$  image was acquired in all cases (on both scanners) to correct for B0 field inhomogeneities.

Isotropic T1-weighted magnetization-prepared acquisition gradient echo (MPRAGE) images were also acquired from all participants with the following parameters on both scanners: TR/TE = 1900/2.5 ms, inversion time = 900 ms, flip angle =  $9^\circ$ , voxel size =  $0.9 \text{ mm}^3$  and acquisition matrix  $256 \times 256 \times 192$ . Intracranial volume was computed from T1-weighted images using SPM12.<sup>22</sup>

## Diffusion-weighted image processing

All DWI data were pre-processed and analyzed primarily using MRtrix3,<sup>23</sup> with several specific tasks deferred to other software as described below.

DWI data from all participants were pre-processed before analysis. Data were first denoised,<sup>24</sup> after which Gibbs ringing artefacts were removed.<sup>25</sup> Susceptibility distortion correction, eddy-current and motion correction were then performed using FSL's 'topup' and 'eddy' tools (version 6.0).<sup>26-28</sup> Bias field correction was then performed based on the mean  $b = 0$  image using ANTs (Advanced Normalization Tools) N4,<sup>29</sup> and DWI images were upsampled to a voxel size of 1.3 mm<sup>2</sup> using cubic b-spline interpolation.

Following these pre-processing steps, fibre orientation distribution functions (ODFs) were computed using single-shell 3-tissue constrained spherical deconvolution (SS3T-CSD),<sup>30</sup> using group-averaged response functions for WM, grey matter (GM) and CSF.<sup>31,32</sup> Joint bias field correction and intensity normalization were then performed.<sup>33,34</sup>

A 'healthy' population template image was generated using WM ODF images from a subset of 20 healthy control participants selected randomly from the control cohort, using an iterative registration and averaging approach.<sup>35</sup> Spatial correspondence was achieved by registering WM ODF images from all participants (controls and patients) to this template using ODF-guided non-linear registration.<sup>35,36</sup>

A whole-brain tractogram was generated using probabilistic tractography on the population template image. Twenty million streamlines were generated, after which the SIFT (Spherical-deconvolution Informed Filtering of Tractograms) algorithm was applied to filter the tractogram to 2 million streamlines to reduce reconstruction biases.<sup>37</sup>

We then applied the FBA<sup>20</sup> framework, where the term 'fixel' refers to a specific fibre population within a single image voxel. Different voxels within an image may contain a different number of fixels. These are computed based on segmentation of the WM ODFs<sup>37</sup> with correspondence established between subject-specific fixels and those of the WM ODF template.<sup>20</sup> A measure of fibre density and cross-section (FDC) was obtained at each WM fixel in the population template space for all participants. This FDC metric combines microstructural and morphological information, such that it is sensitive to changes in the density of fibres passing in a particular direction within a given voxel, as well as the changes in the cross-section of fibre bundles that traverse multiple image voxels.<sup>20</sup> Connectivity-based smoothing was performed on fixel-based measures for all participants.<sup>38</sup>

## Fibre-tract extraction

Major fibre tracts of interest were delineated on the WM ODF template using TractSeg.<sup>39</sup> Tracts of interest were selected for analysis based on having previously exhibited abnormality in group studies comparing epilepsy patients to control cohorts were selected for analysis. These tracts were: the arcuate fasciculus (AF), corpus callosum (CC), cingulum bundle (CG),

CST, fornix (FX), inferior fronto-occipital fasciculus (IFOF), inferior longitudinal fasciculus (ILF), superior cerebellar peduncle (SCP), three segments of the superior longitudinal fasciculus (SLF I, II and III) and uncinate fasciculus (UF). With the exception of the CC, all tracts were bilateral (one left hemisphere tract and one right hemisphere tract).

Delineated fibre tracts were then converted into fixel masks using the 'tck2fixel' command in MRtrix3,<sup>23</sup> and subsequently thresholding this fixel image to create a binary tract fixel mask. The mean FDC value across all fixels within each tract-of-interest was computed for each participant. Given that DWI data from patients included in this study were acquired from two different scanners, we first performed tract data harmonization using ComBat.<sup>18</sup> Following this, assumptions of normality were tested for each tract across the healthy control cohort, after which rank-based inverse normal transformations (INTs) were applied.

## Statistical analysis

### Tract-level analysis

The mean and standard deviation (SD) of tract FDC were computed across the healthy control cohort for each WM tract. Following this, Z-scores were calculated for individual patients with epilepsy when compared to the healthy control cohort. Spider plots were used to display tract Z-scores for individual patients across all tracts. The pipeline for individual tract-based analysis is shown in Fig. 1.

A summary laterality index (LI) was computed using the respective sums of all Z-scores across all tracts in each hemisphere:  $LI = (L_{sum} - R_{sum}) / (L_{sum} + R_{sum})$ .

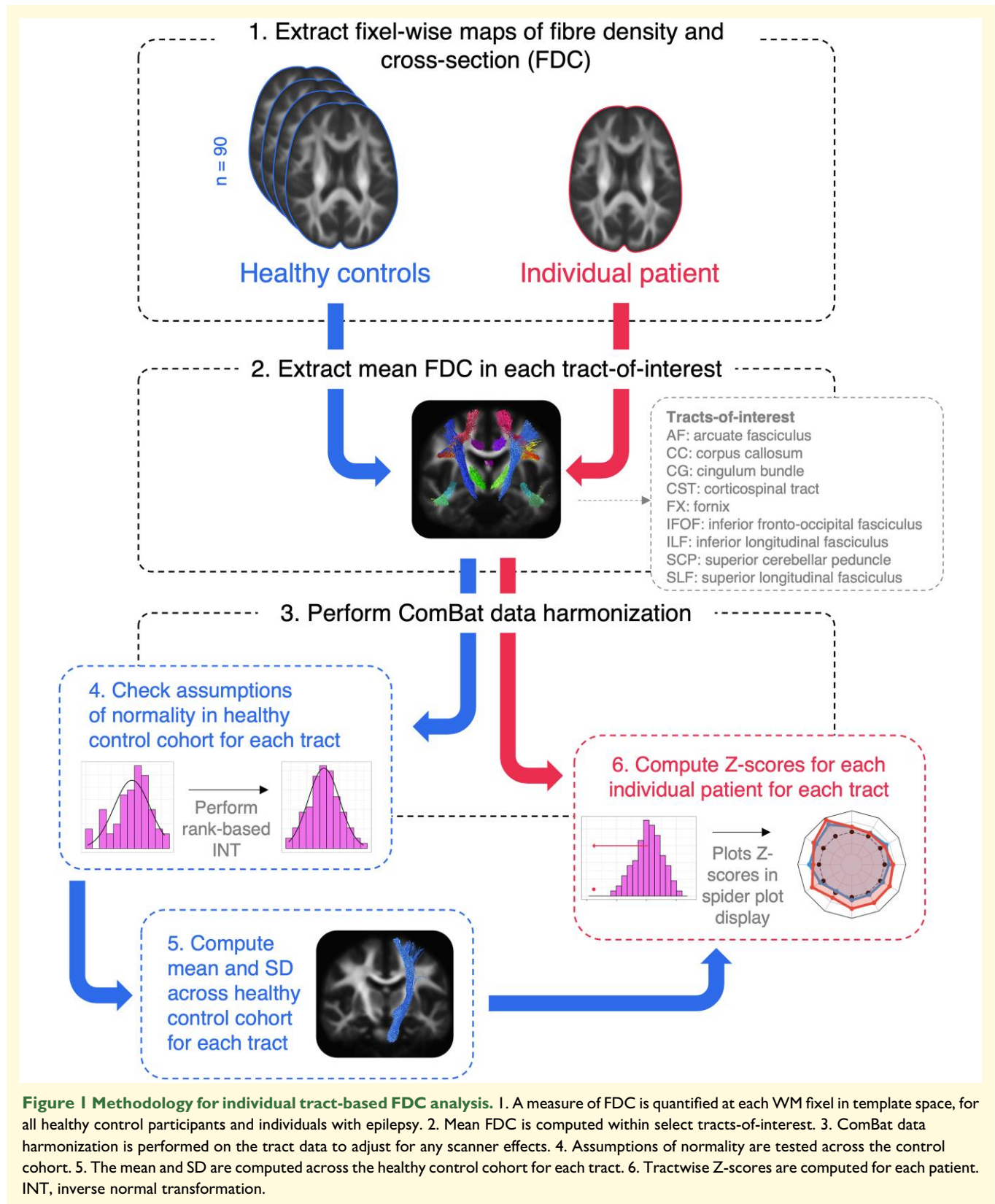
All tract-level analysis was performed in R statistical software (version 3.6.3). Packages utilized include the 'neuroCombat' package for tract data harmonization, 'RNOMni' package<sup>40</sup> to perform rank-based INTs, and 'fmsb' package<sup>41</sup> for generation of spider plots. The code to perform analysis and generate plots is available in R, along with tract data from this study (<https://github.com/remikamito/spidey>).

### Fixel-level analysis

Subject-specific deviations from the healthy control population were also explored at the level of each individual WM fixel. Here, a similar pipeline to the tract-based approach was implemented, whereby the healthy population FDC mean and SD were computed at each WM fixel. Z-scores were then calculated at each template fixel for each epilepsy patient to create a Z-map of fixel-level deviations compared to the control cohort.

## Results

The results of the individualized fixel analysis framework are illustrated with 10 case studies. Table 2 summarizes the key findings for each patient, including a summary LI for tract-based results, and WM regions that exhibited decreased FDC in the whole-brain fixel-level maps. As expected, individual patients with epilepsy exhibited highly variable patterns of WM abnormality compared to the healthy control cohort,



both at the tract-level and fixel-level. [Figure 2](#) is a demonstration of the spider plot display that is used to present patient tract-level results in [Figs 3–5](#) (data from Patient 1).

### Patients 1–4: temporal lobe epilepsy

[Figure 3](#) shows the tract- and fixel-level results for the four patients with TLE (Patients 1–4). Patient 1 is an individual with

**Table 2** Key tract-level and fixel-level findings for each patient

Patient	Tract-level findings			Key fixel-level findings
	Tract Z-score laterality index <sup>a</sup>	Most affected tract	Smallest Z-score	
1	0.1538	Left IFOF	-2.13	Relatively extensive WM abnormalities in fixels within temporal lobe (L > R) and association fibre pathways connecting into L inferior frontal lobe, along with thalamocortical pathways bilaterally
2	-0.136	Right UF	-2.73	Some diffuse WM abnormalities bilaterally, but with greatest cluster of abnormality within right temporal lobe and connecting into thalamic structures
3	-0.258	Left UF	-1.00	Small clusters of diffuse abnormality, including small areas within right temporal lobe extending into inferior frontal lobe, along with left inferior frontal cluster
4	0.063	Left cingulum	-1.22	Some diffuse WM abnormalities in temporal lobes bilaterally (L > R), along with bilateral thalami and splenium of CC
5	0.028	Left SCP	-2.74	Focal, bilateral WM abnormality in cerebellar WM
6	0.018	Right CST	-2.79	Extensive and bilateral WM abnormality throughout most brain WM
7	0.393	Left FX	-2.26	WM abnormalities in left CG, splenium of CC and bilateral fornices and surrounding posterior horn of lateral ventricles (L > R), and left medial temporal lobe
8	-1.594	Right AF	-2.04	Right hemisphere WM abnormality within temporal lobe, WMWM surrounding posterior horn of lateral ventricle and extending into parietal WM superiorly
9	-0.163	Right CST	-2.19	Major focus of WM abnormality in right inferior parietal/posterior frontal WM surrounding post-central sulcus
10	0.121	Left SCP	-0.83	No sizeable clusters of WM abnormality observed, although some diffuse subtle abnormalities observed in right central sulcus and right superior cerebellar WM

<sup>a</sup>Positive values indicate L > R abnormality; Negative indicates R > L abnormality. Tract laterality is computed across all included tracts in each hemisphere.

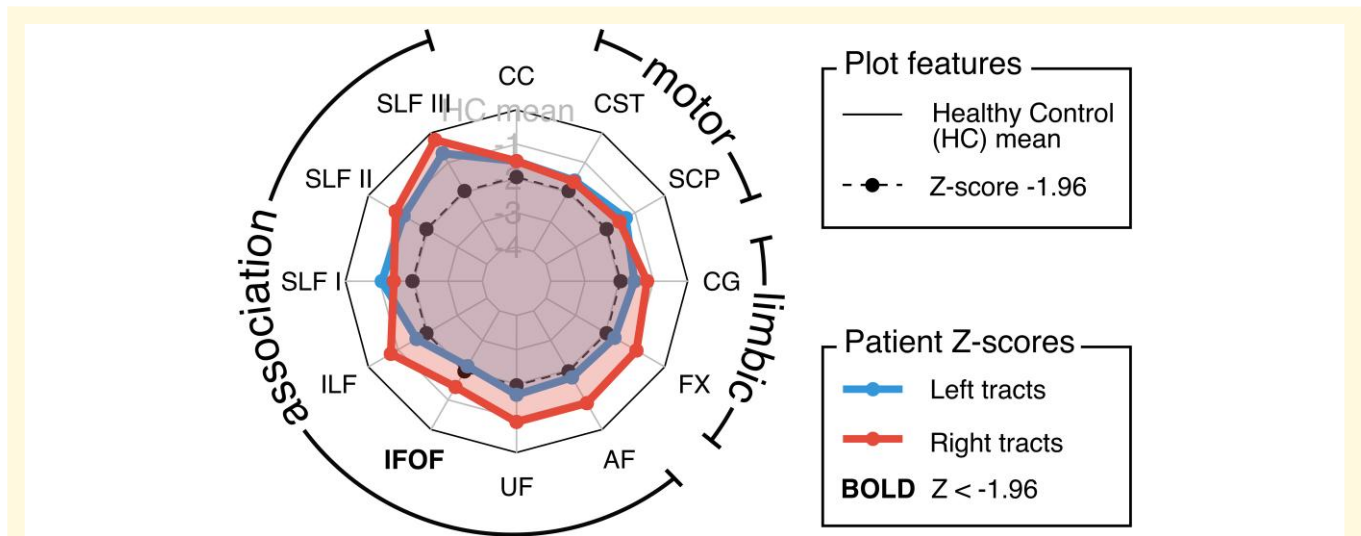


**Figure 2** Exemplar spider plot display for tract z-scores in an individual patient (patient 1). Z-scores are plotted for an individual patient ( $n = 1$ ) in a spider plot display. Each data point represents the Z-score for a given tract in the individual patient, with Z-scores for left hemisphere tracts shown on the lower layer (in blue) and Z-scores for right hemisphere tracts shown on the upper layer (in red). The inner dotted line (and corresponding data points in black) reflects a Z-score of  $-1.96$ , and outer solid line reflects the healthy control mean. The solid grey lines correspond to Z-scores of  $-1$ ,  $-2$ ,  $-3$  and  $-4$ , with greater magnitude (more negative) scores toward the centre of the plot. The CC is included at the top centre, and the Z-score for this tract is included in both left and right hemisphere spider plots. Tracts with a Z-score of  $< -1.96$  in either hemisphere are labelled in bold. AF, arcuate fasciculus; CC, corpus callosum; CG, cingulum; CST, corticospinal tract; FX, fornix; IFOF, inferior fronto-occipital fasciculus; SCP, superior cerebellar peduncles; SLF, superior longitudinal fasciculus; UF, uncinata fasciculus.

severe left HS and recurrent focal dyscognitive seizures. Patient 2 is an individual with right TLE due to HS. Patient 3 is an individual with MRI lesion-negative right TLE (LN-RTLE). Patient 4 is an individual with lesion-negative left TLE (LN-LTLE).

In patients with TLE and HS (Patients 1 and 2), tract-level spider plots demonstrate predominantly ipsilateral abnormality of tracts related to the temporal lobe (Table 2), with the greatest FDC reductions in the UF, AF, ILF and IFOF. Fixel-level

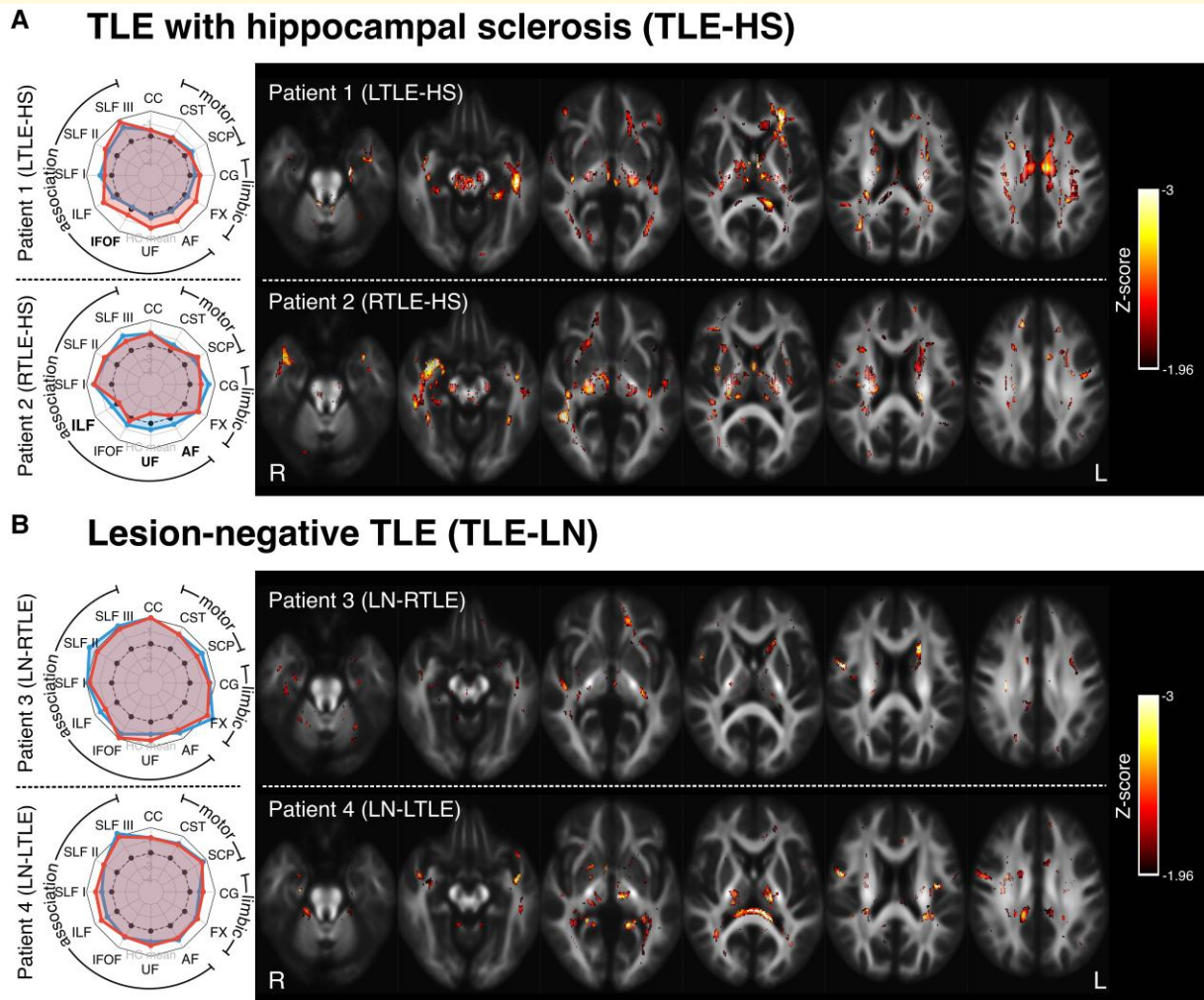


**Figure 3** Tract- and fixel-level results for four patients with TLE. **(A)** Two patients with HS: Patient 1 is an individual who has left TLE with HS (L TLE-HS); Patient 2 is an individual with right TLE with HS (R TLE-HS). **(B)** Two patients with LN TLE: Patient 3 is an individual with MRI-negative or LN-RTLE; and Patient 4 is an individual with LN-LTLE. In all cases, spider plots on the left show Z-scores for FDC measures in each tract-of-interest (see Fig. 2 for interpretation). Fixel-level Z-score maps are shown on the right, with fixels exhibiting a Z-score of  $-1.96$  or greater. Axial slices are placed at 10 mm increments. AF, arcuate fasciculus; CC, corpus callosum; CG, cingulum; CST, corticospinal tract; FX, fornix; IFOF, inferior fronto-occipital fasciculus; SCP, superior cerebellar peduncles; SLF, superior longitudinal fasciculus; UF, uncinate fasciculus.

abnormalities were greatest in the affected medial temporal lobe for both patients (left for Patient 1, right for Patient 2).

The patients with LN TLE (Patients 3 and 4) had milder but diffuse bilateral tract changes, with slightly greater tract abnormality ipsilateral to the epileptic side. Fixel-level findings did not indicate any striking focal abnormalities in these two individuals.

### Patients 5 and 6: progressive myoclonus epilepsy and dravet syndrome

Figure 4 shows tract and fixel-level results for two examples of patients with specific epilepsy syndromes: progressive myoclonus epilepsy (PME) and Dravet syndrome.

Patient 5 is an individual with PME with reasonable cognitive function. PME is commonly associated with cerebellar abnormalities, and the tract-level analysis revealed striking bilateral abnormality within the SCP, with minimal

deviation from the norm in most other fibre tracts. The fixel-level Z-score map similarly exhibited focal abnormality within cerebellar WM.

Patient 6 is an individual with severe Dravet syndrome and intellectual disability. Both tract-level and fixel-level FDC measures exhibited widespread abnormality across most WM fibre tracts.

### Patients 7–10: malformations of cortical development

Figure 5 shows both tract-level spider plots and fixel-level findings in patients with malformations of cortical development (MCDs; Patients 7–10). Patient 7 is an individual with focal dyscognitive seizures due to PVNH surrounding the left lateral ventricles. Patient 8 is an individual with focal epilepsy due to PVNH and PMG within the right temporal lobe. Patient

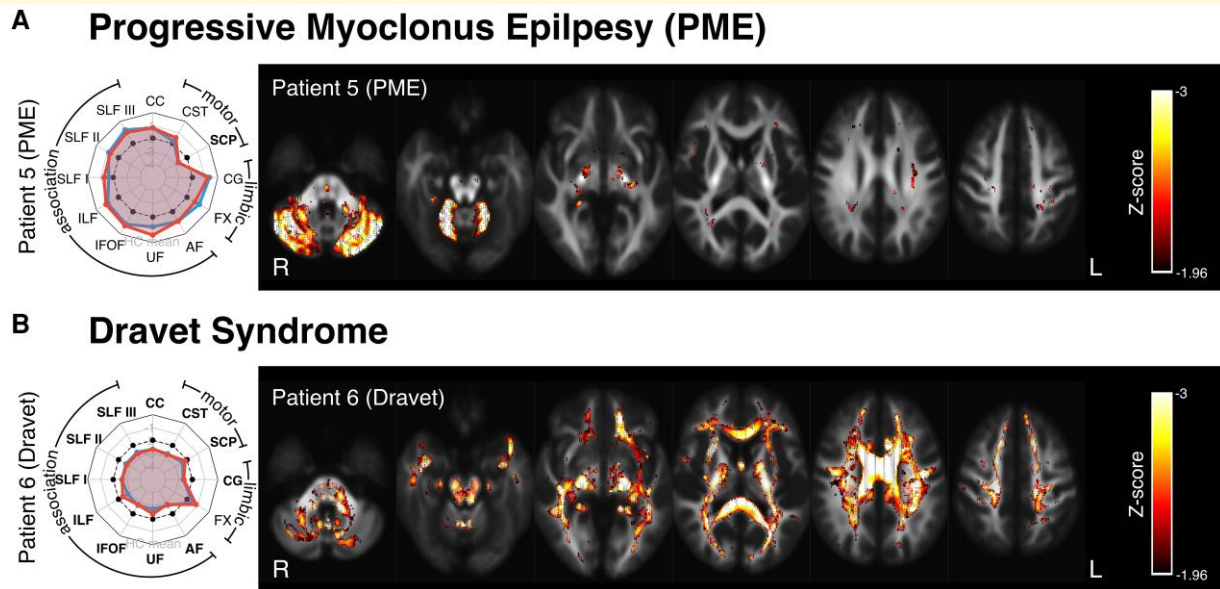


**Figure 4 Results in syndromic epilepsies.** (A) Patient 5 is an individual with PME. (B) Patient 6 is an individual with Dravet syndrome. As with Fig. 3, spider plots are displayed on the left, showing tract-based Z-scores, while fixel Z-maps are displayed on the right (see Fig. 2 for spider plot interpretation). Axial slices are placed at 15 mm increments. AF, arcuate fasciculus; CC, corpus callosum; CG, cingulum; CST, corticospinal tract; FX, fornix; IFOF, inferior fronto-occipital fasciculus; SCP, superior cerebellar peduncles; SLF, superior longitudinal fasciculus; UF, uncinate fasciculus.

9 is an individual with a small bottom-of-sulcus dysplasia (BOSD) in the right precentral sulcus, and Patient 10 is an individual with a small BOSD in the right post-central sulcus.

In all patients, the tract LI indicated greater tract abnormality on the side ipsilateral to the respective lesion(s). Tract-level findings also appear to reflect the clinical or cognitive profiles in these individuals: for example, in Patient 8, left hemisphere tracts appear normal while there is notable right hemisphere WM abnormality, in keeping with the cognitive profile for this individual, who had normal intellect but some non-verbal memory deficits.

In most cases, either the most affected tract or the pattern of tract-level changes provided some indication of the spatial location of the structural epileptogenic abnormality; however, tract-level changes were of insufficient granularity to identify the focal lesion, particularly in the two cases with BOSD. Importantly, fixel-level Z-maps provided finer grain detail, exhibiting patterns of WM abnormality that were concordant with the epileptogenic lesions. In the two patients with highly focal BOSD, although Patient 9 exhibited a striking fixel-level finding that was spatially concordant with the epileptogenic lesion (right precentral sulcus BOSD), Patient 10 exhibited only subtle WM changes, with small foci of decreased FDC and only a small cluster of potentially concordant change in the right central region near the lesion (right post-central BOSD).

## Discussion

We present an advanced diffusion MRI approach quantifying WM abnormalities in individual epilepsy patients, by adapting

the FBA framework to individualized assessment. This approach provides proof-of-principle evidence of the potential clinical use of this advanced diffusion MRI technique in epilepsy. In this case series, we show individual-level findings of tract- and fixel-specific change in patients with varying types and causes of epilepsy (TLE, PME, Dravet syndrome and MCDs). We demonstrate that patients with epilepsy exhibit variable patterns of WM abnormalities and that these WM changes are concordant with the clinical profile of these patients.

## Individualized white matter abnormalities reflect syndrome-specific patterns

In this study, we assessed fixel-based metrics in 10 patients with varying epilepsy causes and syndromes. This enabled the identification of individualized differences within white matter fibre tracts when compared to a control cohort. The patterns of WM abnormality in these patients appeared concordant with the specific epilepsy syndrome or cause in each individual. However, patient-level variability was also observed, highlighting potentially heterogeneous WM profiles across individuals, particularly in those with spatially distributed focal lesions.

For the patients with TLE, variable patterns of WM abnormality were observed, in line with the distinct TLE subtypes of these patients. Although WM abnormalities appeared particularly marked within the temporal lobe ipsilateral to the lesion in the two patients with HS, they also extended beyond the affected temporal lobes. The tract-specific decreases in FDC were

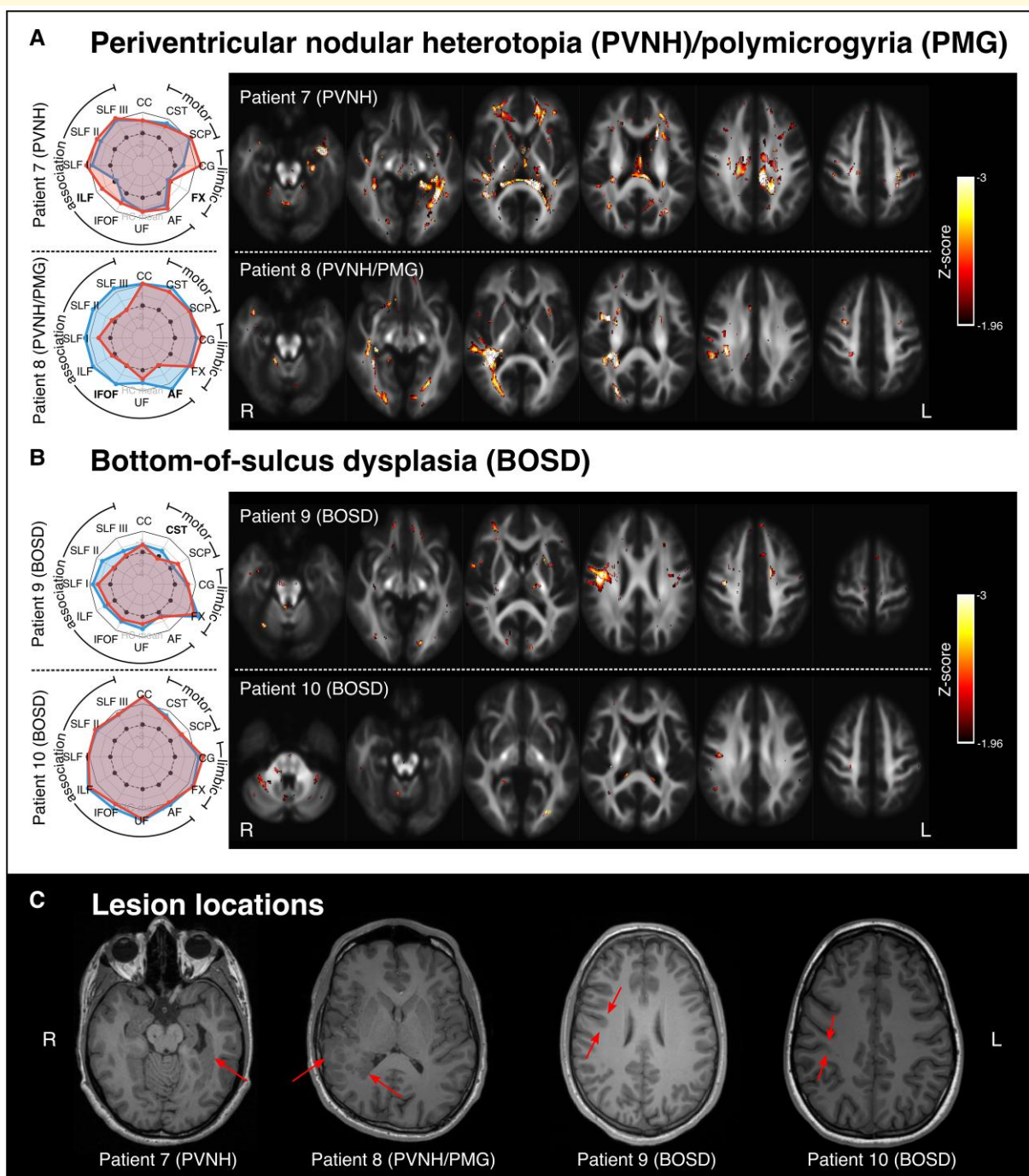


**Figure 5 Results in lesional epilepsies.** (A) Pane shows individual-level results for two patients with PVNH, one with additional PMG. In both cases, lesions were unilateral, with Patient 7 exhibiting left-sided PVNH, and Patient 8 exhibiting right-sided PVNH and PMG. (B) Panel shows individual-level results for two patients with BOSD: Patient 9 had a small BOSD in the right precentral sulcus; Patient 10 had a BOSD in the right post-central sulcus. See Fig. 2 for spider plot interpretation for Panels A and B. (C) Panel shows the lesion locations for all patients (Patients 7–10) on a single axial slice from a T1-weighted image in each subject's own space.

more marked in the two patients with HS (Patients 1 and 2), than in the two LNTLE patients, who exhibited relatively minimal WM abnormality. This is consistent with group-level findings, which have demonstrated more extensive patterns of abnormality in patients with HS than in MRI-negative TLE, both within WM<sup>2,4,5</sup> and in the cortex.<sup>42,43</sup> However,

these differences have been suggested to be influenced by clinical characteristics such as disease duration.<sup>2</sup> Of note, both MRI-negative TLE patients in our study had a later age of onset and shorter disease duration than the two TLE-HS patients, and the difference in extent of WM abnormalities may reflect these clinical characteristics.

In contrast to the patients with TLE, the two patients with specific epilepsy syndromes associated with generalized seizure types exhibited much more bilateral patterns of WM abnormality. The patient with PME exhibited a highly cerebellar signature in their pattern of WM abnormality. Patients with PME exhibit progressive neurological dysfunction, including cerebellar ataxia, and the causes of PME are often associated with cerebellar pathology that is absent in the cerebrum.<sup>44</sup> The pattern of tract-specific WM abnormality in the PME patient included in this study (Patient 5) suggested a marked cerebellar focus on this individual's pathology, which is concordant with the clinical signature of PME. Although this individual did not have the more common form of Unverricht-Lundborg Disease (ULD), a group study in ULD using DTI has similarly demonstrated cerebellar, subcortical and thalamocortical WM changes.<sup>45</sup>

Dravet Syndrome is a severe drug-resistant epilepsy syndrome characterized by generalized tonic-clonic seizures, often with intellectual disability. The patient with Dravet syndrome (Patient 6) exhibited widespread abnormality in WM tract FDC, with virtually all tracts of interest exhibiting substantial decreases in FDC, and much of the brain's WM being implicated at the voxel-level. This finding is in line with the marked WM changes demonstrated at a group level using FBA,<sup>46,47</sup> which may result from abnormal axonal growth in Dravet syndrome, as shown in animal models.<sup>48</sup>

The individuals with malformations of cortical development exhibited highly patient-specific changes. In three of these four individuals (Patients 7–9), the pattern of WM abnormality was spatially concordant with the identified seizure-causing structural abnormality. Patients 7 and 8, who had unilateral PVNH (with additional PMG in Patient 8), exhibited WM abnormalities in a highly lateralized manner, with the most notable abnormalities in the WM proximal to the heterotopic lesions. Patient 9 exhibited focal abnormality in the right precentral region, spatially concordant with the epileptogenic BOSD in this individual, while Patient 10, who had somewhat more subtle BOSD in a spatially proximal area (right post-central region), did not show any notable WM changes.

These individual findings were somewhat in contrast to previous group-level analyses. Group studies comparing patients with malformations of cortical development to healthy control cohorts have typically shown WM changes that extend beyond the MRI-visible lesions.<sup>4,6,49–54</sup> In the case of BOSD patients, we recently showed that despite spatial heterogeneity in the location of the epileptogenic lesions, patients exhibited a typical pattern of bilateral structural network abnormality.<sup>6</sup> These bilaterally distributed WM changes have been suggested to reflect the secondary effect of epilepsy on the brain,<sup>6,52</sup> rather than primary pathology in these patients, given the heterogeneous distribution of these lesions. In group-level analyses, we are likely sensitive to such seizure-affected WM changes, which may be common to patients within an otherwise quite heterogeneous group, while being largely desensitized to subject-specific abnormalities. On the other hand, individual-level

abnormalities are likely to be more marked in the area immediately proximal to these epileptogenic lesions and may be more clinically meaningful than group-level findings.

## Clinical significance of individual tract-specific analysis

An important consideration in MRI studies in epilepsy, particularly in patient cohorts with spatially varied pathology, is the heterogeneity within patient groups. Group-based studies inherently compare group means, which enables identification of co-localized effects between subject groups, but disregards individual-level differences outside these co-localized regions as noise. Neuroimaging studies over the past decade, including large collaborative studies,<sup>2,42</sup> have predominantly focused on group-level analyses that demonstrate common brain changes in patients with varying types and causes of epilepsy.

There is growing interest in moving from group-level studies to individualized neuroimaging analysis and prediction in epilepsy.<sup>55</sup> This is particularly pertinent for precision medicine in epilepsy, where neuroimaging plays a key role in diagnosis and clinical management. To meet this need, neuroimaging techniques must offer clinically valuable insights at an individual-patient level. This study examined whether WM abnormalities in individual patients with varying types and causes of epilepsy offer clinically insightful information, and translate an advanced diffusion MRI tool into the individual-patient level.

In light of our findings, we believe the clinical significance of this individual-level FBA is 2-fold. First, tract-specific WM changes may provide insight into the underlying epilepsy type or syndrome, and we may be able to detect patterns of WM disruption that are diagnostically useful. Second, individual-level Z-score maps of fibre-tract-specific abnormality may help to localize focal epileptogenic abnormalities, particularly in cases where these abnormalities are highly subtle (e.g. in BOSD).

We note that our study is not the first to investigate WM abnormalities in individual patients with diffusion MRI. As with group-level analyses, studies examining WM abnormalities in individual patients with epilepsy have typically adopted the diffusion tensor model, demonstrating subject-specific microstructural abnormalities.<sup>49,56</sup> However, DTI-based results are inherently voxel-averaged or voxel-aggregated, rendering them potentially sensitive, though not specific to underlying fibre structures.<sup>15,57</sup> Although advanced diffusion MRI methods have similarly been applied to probe microstructural changes,<sup>11,58</sup> these studies have also depended on measures that are quantified on a per-voxel basis.

Importantly, by implementing an FBA approach, this work moves beyond voxel-averaged measures to a fibre-tract-specific model.<sup>20,59</sup> This approach enables more comprehensive insight into WM changes within specific fibre populations, as has been demonstrated extensively in many group-level analyses.<sup>60</sup> Reported changes to the derived metrics (namely, FDC) can therefore be ascribed to specific fibre tracts. In this work, we demonstrate that this advanced diffusion MRI approach can

be extended to applicability at an individual-patient level, and in doing so, can offer important clinical insight into the specific fibre tracts that may be affected in individuals.

## Limitations and future directions

Despite the promise of this individualized approach, there are limitations to this work. This study should be considered proof-of-principle, underscoring the importance of developing a methodological approach for detecting individual tract-specific changes. As such, we included a set of epilepsy patients ( $n = 10$ ) with variable causes of epilepsy to gauge the types of patients for whom these individualized analyses may be helpful in future. We also selected patients from retrospective cohorts who exhibited well-characterized clinical signs typical of their epilepsy diagnosis, which may contribute to some selectivity bias. It is important to note that, unlike group-level analyses, improvements in statistical power cannot be achieved in this approach by including a greater number of patients. However, future studies with larger cohorts will provide a clearer picture of individual changes in WM in epilepsies, both within and across diagnoses, and this work may be considered a pilot study for such larger cohort studies. To this end, the code and data used to generate individualized tract-based changes are included in this work. Future work should systematically test individual-level tract changes in a large cohort of epilepsy patients, including those with complex or atypical aetiology, to determine the clinical utility of this technique.

In this work, we focused on the spatial localization of any WM changes observed, rather than on quantifying the significance of any effect, and therefore, did not perform stringent statistical corrections for multiple comparisons. It is essential to note that clinical tools at the individual level should focus on quantifying effect size over statistical significance. Setting somewhat arbitrary thresholds for statistical significance (e.g. by performing false discovery rate or familywise error corrections as has been the case in other individualized approaches<sup>61</sup>) runs the risk of disregarding potentially important clinical information; however, the converse of excess false positives may complicate interpretation for clinicians. To this end, approaches that capture variation across multiple clinical and demographic parameters within large control cohorts may be valuable, as they will likely help to identify key deviations that are of biological or clinical importance.

One approach to circumvent the challenges of classical statistical inference methods in individual-patient analysis is to adopt machine learning approaches. In particular, normative modelling approaches that incorporate machine learning models have gained substantial momentum in the last few years, as a means to probe single subject-level deviations against a large normative sample.<sup>62,63</sup> Recent work in other neurological conditions and disorders, including psychiatric disorders<sup>63,64</sup> and dementia,<sup>65</sup> has demonstrated that individual-level brain structural abnormalities can be identified using such normative approaches. To a limited extent, microstructural abnormalities have been demonstrated in patients with focal cortical dysplasia<sup>66</sup> using normative diffusion MRI-based models,

highlighting the approach's potential in epilepsy. Normative modelling approaches can be applied both independently to select measures (e.g. independent Z-scores per tract), or to extract multivariate measures of deviation (e.g. spatial Z-maps across brain measures), and by implementing machine learning algorithms that are trained on normative features, these approaches are likely to be more sensitive to than classical univariate frameworks.<sup>66</sup> However, given that these machine learning approaches rely on computationally expensive training utilizing big datasets, we believe that proof-of-principle or pilot studies such as this will play an important role in firstly validating the potential clinical impact of a given approach prior to generating large-scale models, in order to minimize wasted resources.<sup>67</sup>

## Conclusion

For neuroimaging studies to be implemented in clinical use, it is crucial to quantify brain abnormalities in individual patients, rather than detect group-level differences between patient and control populations. Our study provides proof-of-principle evidence that by using advanced diffusion MRI analysis, we can identify tract-specific WM abnormalities in individual patients with various types of epilepsy. Our findings suggest that individual WM abnormalities could provide clinically useful information, as the observations appear either concordant with the epilepsy syndromes or spatially concordant with structural abnormalities. We believe these findings are a step towards moving imaging techniques from group-level studies to clinical relevance, supporting precision medicine for the individual patient in future. We have released codes for creating individualized plots for Z-statistics to further encourage other research groups to assess the clinical potential of this approach.

## Supplementary material

Supplementary material is available at *Brain Communications* online.

## Acknowledgements

The authors would like to thank all the participants and their families for their involvement in this study. The Florey Institute of Neuroscience and Mental Health acknowledges the strong support from the Victorian Government and in particular the funding from the Operational Infrastructure Support Grant. The authors acknowledge the facilities and scientific and technical assistance of the National Imaging Facility, a National Collaborative Research Infrastructure Strategy (NCRIS) capability, at the Florey Institute of Neuroscience and Mental Health. The authors would also like to thank Professor Alan Connelly for his contributions to data collection, along with his valuable feedback and fruitful conversations, which contributed greatly to this manuscript.

## Funding

We are grateful to the National Health and Medical Research Council (NHMRC) of Australia for their funding support. This project was supported by an NHMRC grant (Grant number: 1091593) and University of Melbourne Early Career Research Grant (RM).

## Competing interests

The authors have no competing interests to declare.

## Data availability

Code and data to perform tract-level analyses described in this study are available at <https://github.com/remikamito/spidey>. Imaging data are not publicly available as it could compromise the privacy of research participants. Derived data supporting the findings of this study are available upon reasonable request from the corresponding author.

## References

- Engel J Jr, Thompson PM, Stern JM, Staba RJ, Bragin A, Mody I. Connectomics and epilepsy. *Curr Opin Neurol*. 2013;26(2):186-194.
- Hatton SN, Huynh KH, Bonilha L, et al. White matter abnormalities across different epilepsy syndromes in adults: An ENIGMA-epilepsy study. *Brain*. 2020;143(8):2454-2473.
- O'Muircheartaigh J, Vollmar C, Barker GJ, et al. Abnormal thalamocortical structural and functional connectivity in juvenile myoclonic epilepsy. *Brain*. 2012;135(12):3635-3644.
- Campos BM, Coan AC, Beltramini GC, et al. White matter abnormalities associate with type and localization of focal epileptogenic lesions. *Epilepsia*. 2015;56(1):125-132.
- Vaughan DN, Raffelt D, Curwood E, et al. Tract-specific atrophy in focal epilepsy: Disease, genetics, or seizures? *Ann Neurol*. 2017;81(2):240-250.
- Mito R, Vaughan DN, Semmler M, Connelly A, Jackson GD. Bilateral structural network abnormalities in epilepsy associated with bottom-of-sulcus dysplasia. *Neurology*. 2022;98(2):e152-e163.
- McDonald CR, Ahmadi ME, Hagler DJ, et al. Diffusion tensor imaging correlates of memory and language impairments in temporal lobe epilepsy. *Neurology*. 2008;71(23):1869-1876.
- Yogarajah M, Powell HWR, Parker GJM, et al. Tractography of the parahippocampal gyrus and material specific memory impairment in unilateral temporal lobe epilepsy. *Neuroimage*. 2008;40(4):1755-1764.
- Bonilha L, Jensen JH, Baker N, et al. The brain connectome as a personalized biomarker of seizure outcomes after temporal lobectomy. *Neurology*. 2015;84(18):1846-1853.
- Keller SS, Glenn GR, Weber B, et al. Preoperative automated fibre quantification predicts postoperative seizure outcome in temporal lobe epilepsy. *Brain*. 2017;140(1):68-82.
- Winston GP, Micallef C, Symms MR, Alexander DC, Duncan JS, Zhang H. Advanced diffusion imaging sequences could aid assessing patients with focal cortical dysplasia and epilepsy. *Epilepsy Res*. 2014;108(2):336-339.
- Duncan JS, Winston GP, Koeppe MJ, Ourselin S. Brain imaging in the assessment for epilepsy surgery. *Lancet Neurol*. 2016;15(4):420-433.
- Winston GP, Yogarajah M, Symms MR, McEvoy AW, Micallef C, Duncan JS. Diffusion tensor imaging tractography to visualize the relationship of the optic radiation to epileptogenic lesions prior to neurosurgery. *Epilepsia*. 2011;52(8):1430-1438.
- Jones DK. Challenges and limitations of quantifying brain connectivity in vivo with diffusion MRI. *Imaging Med*. 2010;2(3):341-355.
- Mito R, Raffelt D, Dhollander T, et al. Fibre-specific white matter reductions in Alzheimer's disease and mild cognitive impairment. *Brain*. 2018;141(3):888-902.
- Pinto MS, Paoletta R, Billiet T, et al. Harmonization of brain diffusion MRI: Concepts and methods. *Front Neurosci*. 2020;14:396.
- Mirzaalian H, de Pierrefeu A, Savadjiev P, et al. Harmonizing diffusion MRI data across multiple sites and scanners. *Springer*. 2015;9349:12-19.
- Fortin JP, Parker D, Tunç B, et al. Harmonization of multi-site diffusion tensor imaging data. *Neuroimage*. 2017;161:149-170.
- Tournier JD, Calamante F, Connelly A. Robust determination of the fibre orientation distribution in diffusion MRI: Non-negativity constrained super-resolved spherical deconvolution. *Neuroimage*. 2007;35(4):1459-1472.
- Raffelt DA, Tournier JD, Smith RE, et al. Investigating white matter fibre density and morphology using fixel-based analysis. *Neuroimage*. 2017;144:58-73.
- Jeurissen B, Leemans A, Tournier J, Jones DK, Sijbers J. Investigating the prevalence of complex fiber configurations in white matter tissue with diffusion magnetic resonance imaging. *Hum Brain Mapp*. 2013;34(11):2747-2766.
- Friston KJ, Ashburner JT, Kiebel SJ, Nichols TE, Penny WD. *Statistical parametric mapping: The analysis of functional brain images*. Academic Press; 2007.
- Tournier JD, Smith RE, Raffelt DA, et al. MRtrix3: A fast, flexible and open software framework for medical image processing and visualisation. *Neuroimage*. 2019;202:116137.
- Veraart J, Fieremans E, Novikov DS. Diffusion MRI noise mapping using random matrix theory. *Magn Reson Med*. 2016;76(5):1582-1593.
- Kellner E, Dhital B, Kiselev VG, Reiser M. Gibbs-ringing artifact removal based on local subvoxel-shifts. *Magn Reson Med*. 2016;76(5):1574-1581.
- Andersson JLR, Sotiropoulos SN. An integrated approach to correction for off-resonance effects and subject movement in diffusion MR imaging. *Neuroimage*. 2016;125:1063-1078.
- Andersson JLR, Skare S, Ashburner J. How to correct susceptibility distortions in spin-echo echo-planar images: Application to diffusion tensor imaging. *Neuroimage*. 2003;20(2):870-888.
- Bastiani M, Cottaar M, Fitzgibbon SP, et al. Automated quality control for within and between studies diffusion MRI data using a non-parametric framework for movement and distortion correction. *Neuroimage*. 2019;184:801-812.
- Tustison NJ, Avants BB, Cook PA, et al. N4ITK: Improved N3 bias correction. *IEEE Trans Med Imaging*. 2010;29(6):1310-1320.
- Dhollander T, Connelly A. A novel iterative approach to reap the benefits of multi-tissue CSD from just single-shell (+ b=0) diffusion MRI data. *Proc Intl Soc Mag Reson Med*. 2016;24:3010.
- Dhollander T, Raffelt D, Connelly A. Unsupervised 3-tissue response function estimation from single-shell or multi-shell diffusion MR data without a co-registered T1 image, eds. *ISMRM Workshop on breaking the barriers of diffusion MRI*. Vol 5. ISMRM; 2016.
- Dhollander T, Mito R, Raffelt D, Connelly A. Improved white matter response function estimation for 3-tissue constrained spherical deconvolution. *Proc Intl Soc Mag Reson Med*. 2019;27:555.
- Dhollander T, Tabbara R, Rosnarho-Tornstrand J, Tournier JD, Raffelt D, Connelly A. Multi-tissue log-domain intensity and inhomogeneity normalisation for quantitative apparent fibre density. *Proc Intl Soc Mag Reson Med*. 2021;30:2472.
- Raffelt D, Dhollander T, Tournier JD, et al. Bias field correction and intensity normalisation for quantitative analysis of apparent fibre density. *Proc Intl Soc Mag Reson Med*. 2017;25:3541.
- Raffelt D, Tournier JD, Fripp J, Crozier S, Connelly A, Salvado O. Symmetric diffeomorphic registration of fibre orientation distributions. *Neuroimage*. 2011;56(3):1171-1180.

36. Raffelt D, Tournier J, Crozier S, Connelly A, Salvado O. Reorientation of fiber orientation distributions using apodized point spread functions. *Magn Reson Med*. 2012;67(3):844-855.
37. Smith RE, Tournier JD, Calamante F, Connelly A. SIFT: Spherical-deconvolution informed filtering of tractograms. *Neuroimage*. 2013; 67:298-312.
38. Raffelt DA, Smith RE, Ridgway GR, *et al*. Connectivity-based fixel enhancement: Whole-brain statistical analysis of diffusion MRI measures in the presence of crossing fibres. *Neuroimage*. 2015; 117:40-55.
39. Wasserthal J, Neher P, Maier-Hein KH. TractSeg-Fast and accurate white matter tract segmentation. *Neuroimage*. 2018;183:239-253.
40. McCaw Z. RNOmni: Rank normal transformation omnibus test. *R Package*. 2019;861.
41. Nakazawa M. Fmsb: Functions for medical statistics book with some demographic data. *R Package Version 06*. 2018;3.
42. Whelan CD, Alhusaini S, O'Hanlon E, *et al*. White matter alterations in patients with MRI-negative temporal lobe epilepsy and their asymptomatic siblings. *Epilepsia*. 2015;56(10):1551-1561.
43. Bernhardt BC, Bernasconi A, Liu M, *et al*. The spectrum of structural and functional imaging abnormalities in temporal lobe epilepsy. *Ann Neurol*. 2016;80(1):142-153.
44. Zupanc ML, Legros B. Progressive myoclonic epilepsy. *The Cerebellum*. 2004;3(3):156-171.
45. Manninen O, Koskenkorva P, Hyppönen J. White matter degeneration with univentricular progressive myoclonus epilepsy: A translational diffusion-tensor imaging study in patients and cystatin B-deficient mice lactar view project MRI contrast view project. *Radiology*. 2013;269(1):232-239.
46. Raffelt D, Parker D, McMahon J, Scheffer I, Connelly A. Decreased apparent fibre density in dravet syndrome. *Proc Intl Soc Mag Reson Med*. 2014;22:1904.
47. Smith R, Parker D, Schneider A, *et al*. Absence of white matter maturation in Dravet Syndrome. *Organisation for Human Brain Mapping (OHBM)*. 2019;25:1714.
48. Richards K, Jancovski N, Hanssen E, Connelly A, Petrou S. Atypical myelinogenesis and reduced axon caliber in the Scn1a variant model of Dravet syndrome: An electron microscopy pilot study of the developing and mature mouse corpus callosum. *Brain Res*. 2021;1751:147157.
49. Eriksson S, Rugg-Gunn FJ, Symms MR, Barker GJ, Duncan JS. Diffusion tensor imaging in patients with epilepsy and malformations of cortical development. *Brain*. 2001;124(3):617-626.
50. Andrade CS, Leite CC, Otaduy MCG, *et al*. Diffusion abnormalities of the corpus callosum in patients with malformations of cortical development and epilepsy. *Epilepsy Res*. 2014;108(9):1533-1542.
51. Rezayev A, Feldman HA, Levman J, Takahashi E. Bilateral thalamocortical abnormalities in focal cortical dysplasia. *Brain Res*. 2018;1694:38-45.
52. Fonseca VC, Yasuda CL, Tedeschi GG, Betting LE, Cendes F. White matter abnormalities in patients with focal cortical dysplasia revealed by diffusion tensor imaging analysis in a voxelwise approach. *Front Neurol*. 2012;3:121.
53. Filippi CG, Maxwell AWP, Watts R. Magnetic resonance diffusion tensor imaging metrics in perilesional white matter among children with periventricular nodular gray matter heterotopia. *Pediatr Radiol*. 2013;43(9):1196-1203.
54. Chang BS, Katzir T, Liu T, *et al*. A structural basis for Reading fluency: White matter defects in a genetic brain malformation. *Neurology*. 2007;69(23):2146-2154.
55. Lee HM, Fadaie F, Gill R, *et al*. Decomposing MRI phenotypic heterogeneity in epilepsy: A step towards personalized classification. *Brain*. 2022;145(3):897-908.
56. Gross DW, Bastos A, Beaulieu C. Diffusion tensor imaging abnormalities in focal cortical dysplasia. *Can J Neurol Sci*. 2005;32(4): 477-482.
57. Widjaja E, Zarei Mahmoodabadi S, Otsubo H, *et al*. Subcortical alterations in tissue microstructure adjacent to focal cortical dysplasia: Detection at diffusion-tensor MR imaging by using magnetoencephalographic dipole cluster localization. *Radiology*. 2009;251(1): 206-215.
58. Lorio S, Adler S, Gunny R, *et al*. MRI profiling of focal cortical dysplasia using multi-compartment diffusion models. *Epilepsia*. 2020; 61(3):433-444.
59. Raffelt D, Tournier JD, Rose S, *et al*. Apparent fibre density: A novel measure for the analysis of diffusion-weighted magnetic resonance images. *Neuroimage*. 2012;59(4):3976-3994.
60. Dhollander T, Clemente A, Singh M, *et al*. Fixel-based analysis of diffusion MRI: Methods, applications, challenges and opportunities. *Neuroimage*. 2021;241:118417.
61. Jolly AE, Bălăeț M, Azor A, *et al*. Detecting axonal injury in individual patients after traumatic brain injury. *Brain*. 2020;143(4): 1158-1176.
62. Marquand AF, Rezek I, Buitelaar J, Beckmann CF. Understanding heterogeneity in clinical cohorts using normative models: Beyond case-control studies. *Biol Psychiatry*. 2016;80(7):552-561.
63. Rutherford S, Kia SM, Wolfers T, *et al*. The normative modeling framework for computational psychiatry. *Nat Protoc*. 2022;17(1):1-24.
64. Lv J, di Biase M, Cash RFH, *et al*. Individual deviations from normative models of brain structure in a large cross-sectional schizophrenia cohort. *Mol Psychiatry*. 2021;26(7):3512-3523.
65. Verdi S, Marquand AF, Schott JM, Cole JH. Beyond the average patient: How neuroimaging models can address heterogeneity in dementia. *Brain*. 2021;144(10):2946-2953.
66. Chamberland M, Genc S, Tax CMW, *et al*. Detecting microstructural deviations in individuals with deep diffusion MRI tractometry. *Nat Comput Sci*. 2021;1(9):598-606.
67. Lacoste A, Luccioni A, Schmidt V, Dandres T. Quantifying the Carbon Emissions of Machine Learning. *arXiv*. 2019. Advance Access published on October 21, 2019, doi: 10.48550/arxiv.1910.09700.